Mullin JW (1993) *Crystallization*, 3rd edn. Oxford: Butterworth-Heineman Ltd.
Myerson AS, ed. (1999) *Molecular Modeling Applications in Crystallization*. Cambridge: Cambridge University Press.
Sherwood J (1969) Defects in organic crystals. *Molecular Crystals and Liquids* 9: 37.
Sloan ED Jr (1990) *Clathrate Hydrates of Natural Gases*. New York: Marcel Dekker Inc.

Biomineralization

D. Volkmer, University of Bielefeld, Bielefeld, Germany

Copyright © 2000 Academic Press

Many organisms have developed sophisticated strategies to direct the growth of the inorganic constituents of their mineralized tissues. Active control mechanisms are effective at almost all levels of structural hierarchy, ranging from the nanoscopic regime – the nucleation of a crystallite at a specific site – up to the macroscopic regime, where the biophysical properties of the mineralized tissue have to be matched to a certain function.

Among the many open questions, one of the most challenging scientific problems is to gain insights into the molecular interactions that occur at the interface between the inorganic mineral and the macromolecular organic matrix. Biogenic crystals often express exceptional habits that are seemingly unrelated to the morphology of the same type of crystals when grown under equilibrium conditions. For the most widespread calcified tissues it is frequently assumed that a structurally rigid composite matrix consisting of fibrous proteins and thereon adsorbed acidic macromolecules acts as a supramolecular blueprint that templates nucleation of the inorganic phase. Subsequent crystal growth proceeds within a specialized compartment which encloses a suitable aqueous microenvironment. The particular composition of solutes, which often comprises a complex mixture of dissolved electrolytes and macromolecules, has a strong influence on the morphology of the crystals. In the course of mineral deposition, growth modifiers may interact with the maturing crystal in different ways: dissolved macromolecules may be adsorbed onto specific crystal faces, thus slowing down or inhibiting deposition rates along certain crystallographic directions. Adsorbed macromolecules may be completely overgrown by the mineral to produce lattice defects or to introduce discontinuities in the crystal texture.

Efforts in trying to separate and mimic aspects of these complex interactions with simple model systems will help to improve our understanding of crystallization processes that are under biological control. A profitable knowledge transfer in the direction of biologically inspired design strategies for building new and improved composite materials can be predicted for the near future.

The following account of biomineralization focuses on two special topics of this wide research field, namely ferritin and mollusc shell mineralization, which are considered here as illustrative examples. For a more comprehensive survey which includes further important types of biominerals (e.g. bone or biogenic structures made of amorphous silica) the reader should consider one of the many excellent monographs and review articles on the subject.

DropBooks

Ferritin: From Iron Storage to Nanoparticle Synthesis

Mineral deposition in the iron storage protein (ferritin) may be regarded as an archetypal biological model for the formation of a nanocrystalline mineral phase within a confined space. The structure and function of ferritin have been reviewed in great detail. Ferritin consists of an oligomeric protein shell (apoferritin) and a core of poorly crystalline Fe(III) oxyhydroxide (presumably ferrihydrite, $5\ Fe_2O_3 \cdot 9\ H_2O$). Iron is temporarily stored within and released from the central cavity of the encapsulating protein shell. The availability of several high resolution three-dimensional structures of apoferritins originating from different organisms provides a reliable basis to discuss possible pathways of iron biomineralization. Current biomimetic strategies to achieve similar properties include mineralization in oil–water microemulsions, block copolymer micelles, or biotechnologically produced capsule-forming proteins.

Apoferritin Structure and Biological Function

Apoferritins with different amino acid compositions have been isolated from eukaryots as well as

Table 1 Characteristics of ferritins

Iron storage protein	*Source*	*Composition*	*Physiological functions*
Ferritins	Vertebrates Invertebrates	24-mer, predominantly heteropolymeric composed of H-, L- and M-chains Core of crystalline ferrihydrite (polydisperse) Fe/P ratio $\geq 10:1$, 1000–3000 Fe(III)/core	Mobile iron storage Iron detoxification Prevention from hydroxyl radical formation
Bacterioferritins	Eubacteria Fungi	24-mer, predominantly homopolymeric Up to 12 haem (cytochome b_{557}) groups Core of amorphous hydrous ferric phosphate Fe/P ratio 1.1 : 1–1.9 : 1, 600–2300 Fe(III)/core	Precursor to magnetite in magnetotactic bacteria

Adapted with permission from Le Brun N, Thomson AJ and Moore GR (1997) Metal centres of bacterioferritins or non haem-iron-containing cytochromes b_{557}. *Structure and Bonding* 88: 103–138

prokaryots (**Table 1**). Sequence similarities of haem-free ferritins and haem-containing bacterioferritins may fall below 20%. However, their quaternary protein structures are almost identical, suggesting that a convergent molecular evolution within different groups of organisms has independently led to an optimal solution for the availability of a mobile temporary iron storage.

While the general physiological effect of ferritin originating from different organisms may differ, it clearly functions as an iron deposit on the molecular scale, owing to several remarkable features:

- the apoferritin creates a confined space which ultimately restricts the maximum size of the inwardly growing mineral phase;
- several anionic residues induce a net negative charge on the inner protein surface which compensates for the positive surface charges of initially formed polycationic Fe(III) oxyhydroxy species;
- the H-chain ferritin subunit contains a ferroxidase centre that catalyses the oxidation of Fe(II) by molecular oxygen to yield Fe(III);
- the L-chain ferritin subunit bears glutamic acid residues in close proximity which point towards the central cavity, thus possibly acting as an active site for crystal nucleation;
- the apoferritin supports long range electron transfer across the protein coat, enabling fast reductive release of Fe(II) ions from the highly insoluble Fe(III) oxyhydroxide mineral.

Apoferritin is built up by 24 structurally complementary subunits that self-assemble to form a hollow shell of an approximate outer diameter of 11 nm. An individual subunit consists of a long 4-α-helix bundle with an additional short α-helix lying at an angle of about 60° to the bundle axis at the C-terminal side of the amino acid chain (**Figure 1**A). At the beginning of apoferritin self-assembly dimers form mainly through a multitude of hydrophobic contacts along the juxtaposed 4-α-helix bundles. The complete apoferritin shell is composed of 12 dimers that form the faces of an imaginary rhombic dodecahedron (Figure 1B). The protein shell encloses

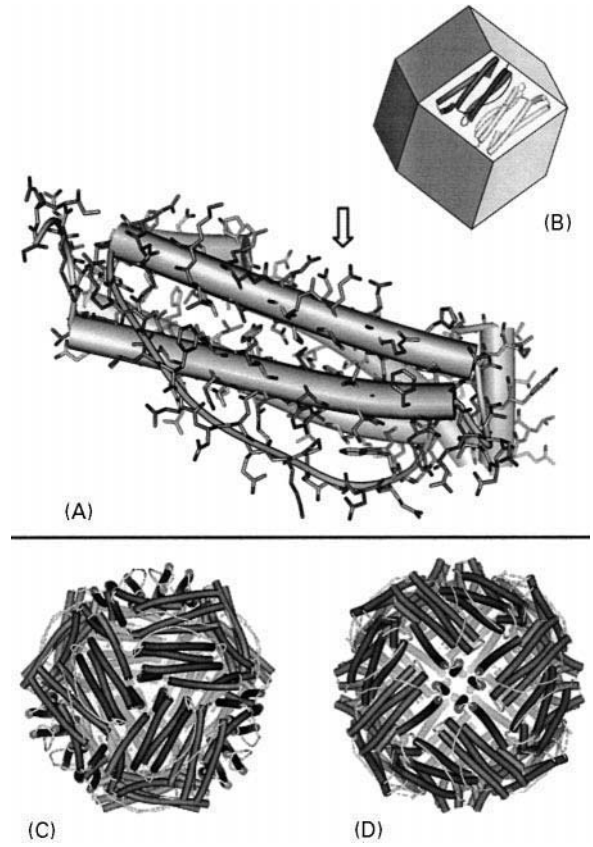

Figure 1 (A) Single apoferritin subunit; α-helix regions of the secondary protein structure are represented as cylinders. The arrow marks a putative mineral nucleation site (here: Glu 57, 60, 61 and 64 of L-chain horse apoferritin, PDB code: 1AEW). (B) Supramolecular architecture of the apoferritin protein shell: 12 subunit dimers form the faces of an imaginary rhombic dodecahedron. (C, D) View along the three-fold channels (the four-fold channels, respectively) of the apoferritin structure. Adapted from Harrison and Arosio (1996).

a nearly spherical cavity of an approximate diameter of 8 nm. The central cavity is accessible through channels of three-fold and four-fold symmetry which are situated at the vertices of the rhombic dodecahedron (Figure 1C, D). While the three-fold channels possess a hydrophilic surface, the four-fold channels are more hydrophobic in nature. The transport characteristics of the ferritin channels are still a matter of controversy. The three-fold channels are likely to be involved in the uptake and release of iron ions as well as in the regulation of the ferritin water content. For the four-fold channels an active role in the uptake of dioxygen has been proposed.

Ferritin Biomineralization

Since ferritin subunits spontaneously self-assemble *in vivo* as well as *in vitro* to yield the complete apoferritin shell, it has been possible to study mineral deposition within the ferritin cavity under various experimental conditions.

Mineral formation within the ferritin cavity proceeds via two different pathways (**Figure 2**): At low iron content, hydrated Fe(II) ions are taken up from the external medium by the H-chain ferroxidase centre where rapid oxidation takes place. Hydrated Fe(III) ions are released from the ferroxidase centre to enter the ferritin cavity (path A). The inner apoferritin surface bears a multitude of primarily hydrophilic and anionic amino acid residues which point towards the central cavity. In particular, each L-chain subunit contains a distinct array of four potentially coordinating glutamate residues (Figure 1A) that could accumulate a small number of hydrated Fe(III) ions. The immobilized Fe(III) ions start to polymerize, leading to an OH^--bridged multinuclear Fe(III) oxyhydroxide cluster. Further cluster growth proceeds via addition of Fe(III) hexaqua cations to the cluster surface with concomitant loss of an H_2O ligand for each established coordinative bond.

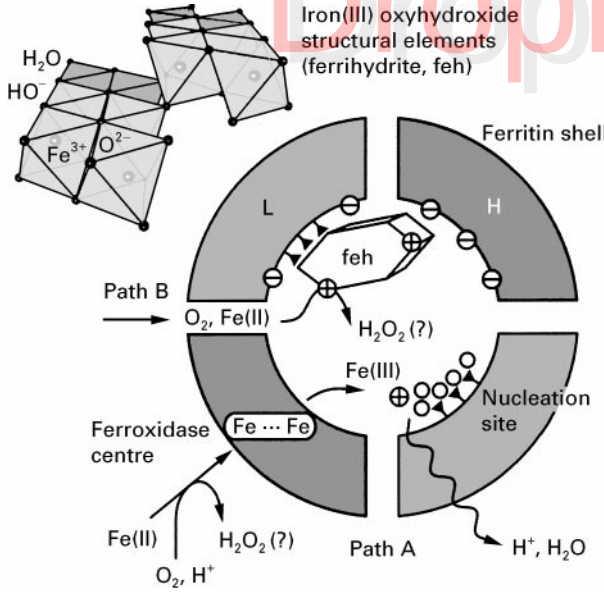

Figure 2 Iron mineral formation in ferritin. A self-assembled heteropolymeric shell forms a spatially confined mineralization compartment composed of H- and L-chain subunits that possess different roles in mineralization. The H-chain contains a preorganized arrangement of coordinating amino acid residues (ferroxidase centre) which is able to take up two Fe(II) ions and to catalyse their oxidation to Fe(III) ions. The L-chain possesses four highly conserved glutamic acid residues, that are assumed to play a decisive role in Fe(III) mineral nucleation.

On reaching a critical crystallite size, autocatalytic Fe(II) oxidation at the surface of the mineral nucleus outweighs ferroxidase-induced oxidation, and mineral growth continues until most of the cavity is filled by one (or several) Fe(III) oxyhydroxide nanocrystal(s) (path B). The pathways of iron transport into the cavity, as well as the primary product(s) of iron(II) oxidation, are not yet fully established.

Since hydrated Fe(III) ions form polycationic oligomers at the initial stages of polymerization, the general consensus is that L-chain glutamate residues contribute to a negative surface potential on the inside of the apoferritin shell in order to create a thermodynamic sink for Fe(III) oxyhydroxide deposition. In addition to this general effect, a more specific template effect on iron mineral formation has been proposed which takes into account the special arrangement of glutamate residues and the fact that the sequence motif is highly conserved among ferritins from different classes of organisms. The poor crystallinity of the ferritin mineral on the other hand, as well as the fact that nanosized Fe(III) oxyhydroxide particles spontaneously grow from Fe(III)-containing aqueous solutions, challenges this interpretation.

Ferritin Core Structure

The mineral phase of ferritin displays properties similar to the iron oxyhydroxide ferryhydrite which is widespread in nature. This mineral has been traditionally described as amorphous or colloidal ferric hydroxide – $Fe(OH_3)$ – due to its poor X-ray diffracting properties. The actual composition however, is $Fe_5HO_8 \cdot 4\ H_2O$ and recent X-ray absorption studies (Fe *K*-edge XANES and EXAFS spectroscopy) have shown that most of the Fe(III) ions are situated in identical, structurally well-defined coordination environments. A highly hydrated ferrihydrite slowly precipitates from Fe(III)-containing solutions at pH ≥ 2 at room temperature. The Fe(III) hexaqua cations

DropBooks

first oligomerize to yield chains of water-soluble polycations in which octahedrally coordinated Fe(III) ions are bridged by hydroxide anions. Further deprotonation and polymerization yield ferrihydrite, which, at close to its zero point of charge at pH 7–8, slowly and irreversibly dehydrates and rearranges to the thermodynamically more stable iron oxide hematite (α-Fe_2O_3). Although the details of the crystal structure and surface properties of ferrihydrite are still controversial, the current data support a structural model in which double chains of edge-sharing iron(III) octahedra are cross-linked via corners (Figure 2, top), similar to the essential structural elements of the mineral goethite (α-FeOOH). The dimensions of coherent X-ray scattering domains for synthetic ferrihydrite are within the range of 1–6 nm, which accounts for the characteristic broadening of X-ray diffraction lines. Temperature-dependent ^{57}Fe Mössbauer spectra of synthetic ferrihydrite and ferritin cores display identical features, indicating a superparamagnetic behaviour of the crystalline phase at room temperature and below. Therefore synthetic ferrihydrite precipitates, as well as ferritin cores, may be better described as nanocrystals rather than nanocolloids.

Biologically Inspired Nanoparticle Synthesis

The intriguing supramolecular architecture of ferritin, as well as its unique functional properties, might be taken as a model for the construction of artificial nanocompartments where crystal growth takes place within a spatially confined microenvironment under controlled conditions. Classical approaches that make use of the entrapped water content of oil–water microemulsions are likewise simple to carry out, but as a rule suffer from relatively broad size distributions of the precipitated nanoparticulate materials. For advanced applications, novel synthetic routes will therefore be required to control the dimensions of the desired inorganic nanoparticles. Examples of technologically important compounds which exhibit strongly size-dependent physical and chemical properties range from catalytically active, highly dispersed metal nanocolloids (e.g. Pt, Pd, Rh), quantum-confined semiconductor nanoparticles (CdS, CdSe) to nanoscale ferrimagnetic particles (e.g. γ-Fe_2O_3) and nanocomposite magnetic alloys. Recent examples of biologically inspired synthetic approaches to synthesize nanoscale inorganic materials include the use of biotechnologically engineered apoferritin shells and virus protein cages (capsids), or the use of monodisperse block copolymer micelles as nanoscale reaction compartments (see Further Reading).

From Calcified Tissues to Engineered Crystals

While ferritin represents an example of a nanosized crystalline biomineral, the architecture for example of a vertebrate bone or a mollusc shell spans several length scales. The morphology of the calcified tissue is ultimately encoded in the genome that governs the biosynthesis of required materials at the cellular level of structural hierarchy. Biomineralization therefore, as a highly complex phenomenon of living organisms, cannot be reduced to a single mechanistic aspect. The following representation of $CaCO_3$ mineralization in molluscs is admittedly a crude simplification which mainly concentrates on structural aspects, while at the same time ignoring the dynamic character of the entire process. Special emphasis here is put on induced $CaCO_3$ crystal nucleation, i.e. the early stages of crystal growth where the system properties can be described by supramolecular recognition events occurring at the mineral–matrix interface. At this level, common features of ferritin, mollusc shell or bone mineralization do exist: the interaction of highly specialized acidic macromolecules with different surfaces of the growing single crystal. Current research efforts focus on the isolation and characterization of macromolecules from calcified tissues. Functional properties of isolated macromolecules or fractions of macromolecules are systematically investigated for their ability to influence $CaCO_3$ nucleation, growth and polymorphism. Biologically inspired synthetic strategies try to assemble artificial matrices in order to mimic structural and functional properties of mineralizing tissues.

Crystallochemical Aspects of $CaCO_3$ Biomineralization

$CaCO_3$, together with amorphous silica, is the most abundant biomineral. There exist three $CaCO_3$ polymorphs – calcite, aragonite and vaterite – all of which occur in calcified tissues. A monohydrate (monohydrocalcite) and a hexahydrate form (ikaite) of $CaCO_3$ have been characterized as metastable precursor phases during the incipient stages of crystal formation (**Table 2**).

At ambient conditions, calcite is the thermodynamically most stable $CaCO_3$ polymorph. However, from oversaturated aqueous solutions containing Mg^{2+} at a molar ratio Mg/Ca > 4 (comparable to the composition of seawater), the only observed crystalline phase is aragonite, while at high supersaturation the metastable polymorph vaterite precipitates from solution.

Table 2 Characteristics of the most important $CaCO_3$ mineral phases

Mineral	*Crystal system (space group)*	*Specific density ($g\ cm^{-3}$)*	*Solubility ($-\log K_{sp}$)*	*Biological occurrence*
Calcite ($CaCO_3$)	Trigonal ($R\bar{3}c$)	2.71	8.48	Very common
Aragonite ($CaCO_3$)	Orthorhombic (*Pmcn*)	2.93	8.34	Very common
Vaterite ($CaCO_3$)	Orthorhombic (*Pbnm*)	2.54	7.91	Rare
Monohydrocalcite ($CaCO_3 \cdot H_2O$)	Trigonal ($P3_121$)	2.43	7.60	Very rare
Ikaite ($CaCO_3 \cdot 6H_2O$)	Monoclinic ($C2/c$)	1.77	7.12	Unknown

Adapted with permission from Morse JW and Mackenzie FD (1990) *Geochemistry of Sedimentary Carbonate*, p. 41. Amsterdam: Elsevier.

The arrangement of the ions in crystalline $CaCO_3$ may be described in terms of separate layers of cations and anions. Coordination environments for Ca^{2+} ions (CO_3^{2-}, respectively) in the polymorphs differ from each other, as a result of different successions of layers, as well as different crystallographic orientations of the planar carboxylate groups in the crystal lattices (**Figure 3**). In calcite, each single densely packed Ca^{2+} layer parallel to the *ab* plane is situated between single layers of CO_3^{2-} with each layer containing anions oriented in opposite directions. Each Ca^{2+} ion is situated in a distorted octahedral coordination environment of six different CO_3^{2-} anions. In aragonite, the positions of Ca^{2+} ions in the *ab* plane are nearly identical to those of the calcite structure. In contrast, the CO_3^{2-} anions below and above the Ca^{2+} layer are separated into two layers, which are lifted by 0.98 Å along the *c* direction, leading altogether to a ninefold coordination of Ca^{2+} ions.

Shell Formation in Molluscs

It has long been recognized that calcifying organisms have developed active mechanisms to select the polymorph, and to control the distribution, shapes and orientations of crystals in their mineralized tissues. Molluscs are among the most thoroughly investigated organisms in this regard; they build concrete shells from $CaCO_3$. The mollusc shell may be regarded as a microlaminate composite consisting of layers of highly oriented $CaCO_3$ crystals which are interspersed with thin sheets of an organic matrix. Crystals within separate shell layers usually consist of either pure aragonite or pure calcite. Vaterite, when present, is usually associated with shell repair. The succession of shell layers, as well as their pronounced ultrastructural features (see **Table 3**) are important characters in mollusc taxonomy. The main protective functions of the shell are to prevent desiccation, predation and abrasion. The shell also provides support for the body and a site for muscle attachment.

Shell formation occurs in two principal phases. The first involves the cellular processes of ion transport and organic matrix synthesis which occurs in different compartments of the molluscan mineralizing system (**Figure 4**A). The second phase comprises a series of crystal nucleation and growth processes taking place in a specialized mineralization compartment,

DropBooks

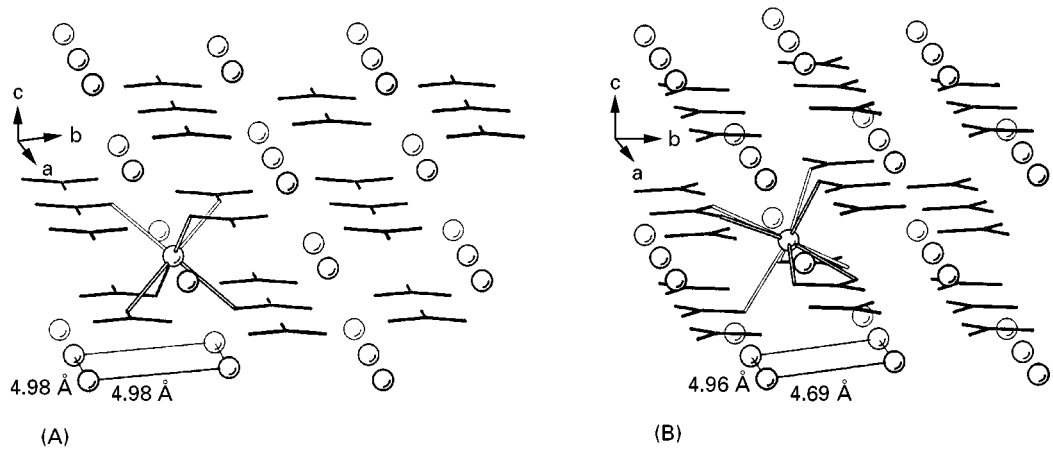

Figure 3 Ion-packing arrangement in the crystal structures of (A) calcite and (B) aragonite. The coordinative bonds between CO_3^{2-} anions (black sticks) and one of the Ca^{2+} ions (open circles) are emphasized with open lines. The minimum distances of Ca^{2+} ions in the *ab* planes for both crystal lattices are indicated at the bottom.

Table 3 Classification of mollusc shell layers

Shell layer	*Composition*	*Ultrastructural characteristics*	*Function*
Periostracum	Thin layer of hydrophobic sclerotized proteins (periostracin) 3,4-Dihydroxyphenylalanine (DOPA) *Asp*-rich proteins, chitin (occasionally)	Outer shell surface Little or no ultrastructural order	Space delineation Protection from corrosion Initial substrate for mineralization Camouflage/protective colouring
Prismatic layer	Calcite or aragonite Water-soluble *Asp*-rich glycoproteins	Outer shell layer extending inward from the periostracum Aggregates of uniformly oriented crystal prisms	Ca^{2+}/HCO_3^- storage Multi-layered architecture
Nacreous layer	Aragonite β-Chitin fibrils, silk fibroin-like (Gly-, Ala-rich) framework proteins Water-soluble *Asp*-rich glycoproteins	Middle or inner shell layer Polygonal, laminar tablets arranged in broad, regularly formed, parallel sheets nearly parallel to the inner shell surface	creates more isotropic structural properties that strengthen the shell against mechanical loading (torsion, fracture)
Foliated layer	Calcite Water-soluble *Asp*-rich glycoproteins Water-soluble phosphoproteins	Lamellae of parallel and elongate blades of crystals dipping uniformly over large portions of the depositional surface	

Adapted with permission from Wilbur KM and Saleuddin ASM (eds) (1983) Shell formation. In: *The Mollusca*, vol. 4, pp. 236–287. San Diego: Academic Press.

the so-called extrapallial space (Figure 4B). Crystals grow in intimate association with a secreted, highly specialized organic matrix. In order for crystals to form, the extrapallial fluid must become supersaturated with $CaCO_3$, which imposes active accumulation strategies upon molluscs that inhibit a freshwater environment, where the external medium is depleted of Ca^{2+} ions. The concentration of Ca^{2+} ions is actively regulated by a Ca membrane transport system that is located in the body and the mantle epithelium. Active carbonate transport has also been postulated for the regulation of HCO_3^- ion concentration. However, as an additional source of hydrogen carbonate, the mollusc may utilize metabolic carbon dioxide from its respiratory system. Any supply of HCO_3^- ions is tightly associated with carbonic anhydrase (CA) activity, an enzyme that catalyses the interconversion of carbon dioxide (CO_2) and carbonic acid (H_2CO_3). High carbonic anhydrase activity is detectable in the extrapallial fluid of molluscs, where the protein seems to be involved in removal of protons from the extrapallial fluid in order to maintain the pH within the appropriate range (7.4–8.3) for mineral formation.

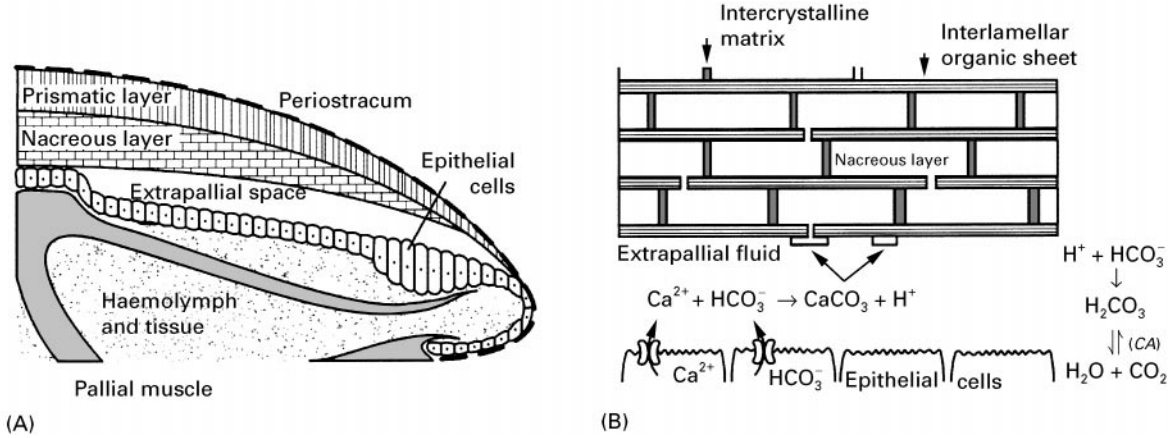

Figure 4 (A) Transverse section of the mantle edge of a bivalve showing the system of compartments. (B) Scheme of ion fluxes at the interface between the outer epithelial cells of the mollusc tissues and the incipient layer of nacre. (Simplified representations, not to scale.)

The extrapallial fluid also contains a complex mixture of inorganic and organic substances. Analysis of several species of marine and freshwater species showed that the major cations present are Na^+, K^+, Ca^{2+} and Mg^{2+} while the major anions are HCO_3^-, Cl^- and SO_4^{2-}. The organic components of the extrapallial fluid include amino acids, proteins, mucopolysaccharides and low molecular organic acids (e.g. succinic acid). The organic compounds are secreted by mantle epithelial cells, but their metabolic origins in mollusc tissue have not yet been located.

The Structure of Nacre

Biogenic crystals may use the inner surface of the periostracum, the surface of other, already formed crystals, or the organic matrix as a substrate. Special attention has been drawn to the microstructure of nacre which exhibits an exceptionally regular arrangement of tabular aragonite crystals. Thin interdigitated aragonite plates develop in close association with thin horizontally aligned organic layers (interlamellar sheets) upon which aragonite crystals are nucleated (**Figure 4**B, **Figure 5**). In order to grow crystals into a highly regular brickwork-like pattern, numerous nucleation events would have to be synchronized with each other at distant locations. An alternative growth mechanism was proposed to explain the precision by which aragonite platelets are uniformly co-aligned within the same and consecutive layers. According to this model, nacre may be constituted of extended, continuous single crystalline domains of aragonite platelets that are interconnecting by mineral bridges through the perforated interlamellar sheets.

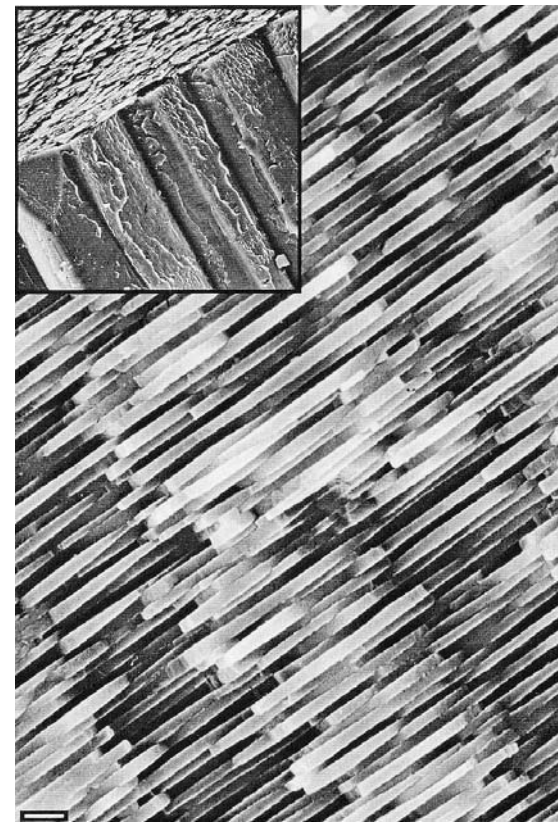

Figure 5 Fractured surface of the nacreous layer of the bivalve mollusc *Atrina rigida*. The inset shows the inner nacreous layer of tabular aragonite crystals (top) and the outer prismatic layer of columnar calcite crystals (bottom). SEM micrographs, scale bar denotes 1 μm. Courtesy of Y. Levi, Department of Structural Biology, Weizmann Institute of Science, Israel.

DropBooks

Biologically Induced Crystal Nucleation

Putative Structure of Acidic Nucleation Sites in Calcified Tissues

One of the critical problems in understanding the mechanisms of matrix-associated mineralization is the lack of information on the three-dimensional structures of biological macromolecules that interface with the mineral. A literature search up to the middle of 1999 yielded very few examples where complete or partial information about the primary structure of macromolecules directly involved in mineralization have been determined (**Table 4**). Macromolecules isolated from mollusc tissues have traditionally been distinguished into two different classes, based on solubility properties. Chemical analysis showed that the insoluble fraction consists mainly of fibrous proteins (collagen, chitin) and/or polysaccharides. These macromolecules together build a rigid framework upon which specific macromolecules from the soluble fraction may become adsorbed. The primary function of the insoluble organic matrix is to subdivide the mineralization compartment into an organized network of microcompartments and thus to delimit the available space for crystal growth and/or to constrain the crystal packing arrangement to a certain extent. The surface of this macromolecular assembly may serve as a supramolecular template for oriented nucleation of single crystals, although this structure–function relation is difficult to prove for biological systems *in vivo*.

The macromolecules contained in the soluble fraction have sequence motifs in common which consist of repeating oligomeric units of acidic residues. Table 4 contains further representative examples of functional macromolecules from calcified tissues. However, the heterogeneity of sources/organisms for isolating these macromolecules, their different

Table 4 Representative structural motifs of macromolecules found in calcified tissues

Name	*Source*	*Repeating oligomeric units*	*Associated mineral*	*Proposed function*	*Reference*
MSI60	Pearl oyster: insoluble protein from the nacreous layer	[Ala_{9-13}] and [Gly_{3-15}]	Aragonite	Framework protein Binding of *Asp*-rich soluble glycoproteins	Sudo *et al*. (1997)
MSI31	Pearl oyster: insoluble protein from the prismatic layer	[Gly_{3-5}] and [*Glu*-Ser-*Glu*-*Glu*-*Asp*-X], (X = Thr or Met)	Calcite	Framework protein Binding of *Asp*-rich soluble glycoproteins	Sudo *et al*. (1997)
MSP-1	Scallop shell: soluble glycoprotein from the foliated shell layer	[*Asp*-Gly-Ser-*Asp*] and [*Asp*-Ser-*Asp*]	Calcite	Induction of oriented nucleation Control of $CaCO_3$ polymorphism	Sarashina and Endo (1998)
Nacrein	Pearl oyster: soluble protein from the nacreous layer	[Gly-X-Asn], (X = *Glu*, Asn, or *Asp*)	Aragonite	Carbonic anhydrase Ca-binding	Miyamoto *et al*. (1996)
Type I collagen	Insoluble fibrous scleroprotein from bone	[Gly-X-Y] triple-helices (X, Y frequently Gly, Hyp)	Hydroxyapatite	Framework protein Binding of acidic regulatory proteins	Prockop and Fertala (1998)
Osteonectin	Acidic glycoprotein from bone	[*Glu*-*Glu*-Thr-*Glu*-*Glu*-*Glu*]	Hydroxyapatite	High affinity Ca-binding Collagen binding	Fujisawa *et al*. (1996)
Phosphophoryn	Soluble highly phosphorylated protein from mineralized dentin	[Ser*-Asp] and [*Asp*-*Ser**-*Ser**] (Ser* = phosphorylated serine)	Hydroxyapatite	Induction of crystal nucleation Regulation of crystal growth Collagen binding	George *et al*. (1996)
PS-2	Acidic polysaccharide from *P. carterae* coccoliths	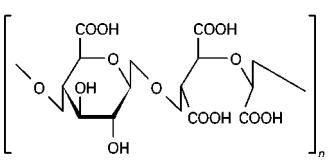	Calcite	Growth modifier Ca-binding	Marsh (1994)

Sudo S, Fujikawa T, Nagakura T *et al*. (1997) Structures of mollusc shell framework proteins. *Nature* 387: 563–564.

Sarashina I and Endo K (1998) Primary structure of a soluble matrix protein of scallop shell: implications for calcium carbonate biomineralization. *American Mineralogist* 83: 1510–1515.

Miyamoto H, Miyashita T, Okushima M et al. (1996) A carbonic anhydrase from the nacreous layer in oyster pearls. *Proceedings of the National Academy of Sciences of the USA* 93: 9657–9660.

Prockop DJ and Fertala A (1998) The collagen fibril: the almost crystalline structure *Journal of Structural Biology* 122: 111–118.

Fujisawa R, Wada Y, Nodasaka Y and Kuboki Y (1996) Acidic amino acid-rich sequences as binding sites of osteonectin to hydroxyapatite crystals. *Biochimica et Biophysica Acta – Protein Structure and Molecular Enzymology* 1292: 53–60.

George A, Bannon L, Sabsay B *et al*. (1996) The carboxyl-terminal domain of phosphophoryn contains unique extended triplet amino acid repeat sequences forming ordered carboxyl-phosphate interaction ridges that may be essential in the biomineralization process. *Journal of Biological Chemistry* 271, 32869–32873.

Marsh ME (1994) Polyanion-mediated mineralization – assembly and reorganization of acidic polysaccharides in the Golgi system of a coccolithophorid alga during mineral deposition. *Protoplasma* 177: 108–122.

chemical nature, and their association with different mineral phases clearly rule out a uniform function. They may roughly be divided into five different functional classes:

- concentration regulators: macromolecules that are linked to Ca^{2+} and/or CO_3^{2-} transport and metabolism (e.g. carbonic anhydrase)
- growth inhibitors: acidic macromolecules that strongly bind Ca^{2+} ions and become nonselectively adsorbed on to any arbitrary crystal face which is exposed to the mother liquor
- growth modifiers: acidic macromolecules that interact stereoselectivity with distinct faces of a nascent crystal
- texture modifiers: acidic macromolecules that become occluded and modify texture and mechanic properties of crystals
- nucleators: immobilized acidic macromolecules that form a highly regular template for induced crystal nucleation

Due to the complex nature of interactions in biological matrices, the same acidic macromolecule may belong to more than one of the above mentioned categories and its functional properties may change within different organisms and microenvironments.

To demonstrate a possible mode of molecular interaction between acidic macromolecules and crystal surfaces, this survey of mollusc mineralization will conclude with a brief section about induced $CaCO_3$ nucleation in biological systems. The body fluids of mineralizing organisms contain crystallization inhibitors that prevent spontaneously formed crystal nuclei from growing into larger crystals. To direct mineral deposition to the appropriate location, active nucleation sites have to exist in mineralizing compartments. The opening section about iron storage has already indicated how the molecular architecture of ferritins may be associated with nucleation of iron minerals. For induced calcite and aragonite nucleation, systematic investigations on biological and suitably assembled artificial systems have shed some light on the structural requirements of a putative nucleation site, especially in mollusc shells. The model of Addadi and Weiner proposes structurally pre-organized domains of acidic residues, that could serve as a supramolecular template for oriented crystal nucleation. Such highly ordered domains could result from acidic macromolecules being adsorbed on a rigid scaffold of insoluble matrix proteins (**Figure 6**). As an example, the interlamellar organic sheets of mollusc shell nacre consist of thin sheets of β-chitin (a water-insoluble (1 → 4)-linked 2-acetamido-2-deoxy β-D-glucan) sandwiched between thicker sheets of silk fibroin-like proteins. Silk fibroin itself possesses microcrystalline

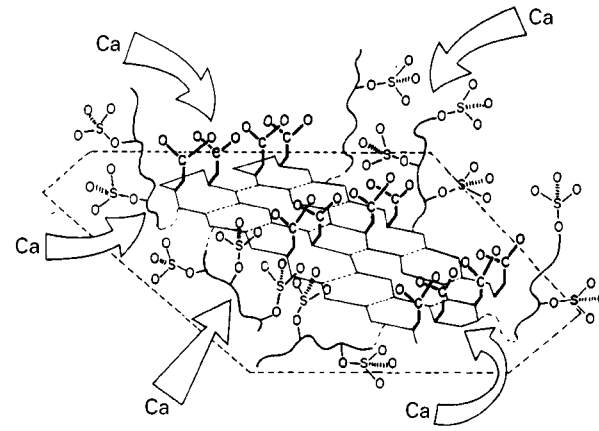

Figure 6 Schematic representation of a putative nucleation site in molluscan tissues. An acidic glycoprotein is anchored to a rigid substrate (as schematized by the broken lines) through hydrophobic or electrostatic interactions. The sulfate groups, linked to flexible oligosaccharide side chains, concentrate Ca^{2+} ions on an *Asp*-rich oligopeptide domain that is assumed to adapt a highly regular β-sheet conformation. A first layer of Ca ions may thus be fixed and oriented in space, upon which further mineral growth ensues. Reproduced with permission from Addadi and Weiner (1989).

domains of repeating $[Gly\text{-}Ala\text{-}Gly\text{-}Ala\text{-}Gly\text{-}Ser]_n$ units that adopt an antiparallel β-pleated sheet conformation. These domains have a highly regular and hydrophobic surface upon which acidic macromolecules are adsorbed from solution. In the course of adsorption, the acidic macromolecules has to fold into the appropriate conformation, in order to maximize its hydrophobic interactions with the silk fibroin surface. Possible candidates for acidic macromolecules interacting with silk fibroin in the described way are oligopeptides that include sequence motifs of $[Asp\text{-}X]_n$, (X = Gly, Ser), which have a strong tendency to fold into a β-sheet conformation in the presence of Ca^{2+} ions. As a consequence, the aspartic acid residues of $[Asp\text{-}X]_n$ sequences would be positioned at only one side of the β-pleated sheet, resulting in an organized two-dimensional array of carboxylate ligands.

It is tempting to assume that the carboxylate residues coordinate a first layer of Ca^{2+} ions which would in turn become the first layer of an epitaxially growing $CaCO_3$ crystal. However, a more profound analysis has so far failed to provide evidence for an epitaxial growth mechanism or a close stereochemical complementarity between the nucleating macromolecules and the incipient $CaCO_3$ crystal surface. Some properties of the mollusc shell ultrastructure rather point to less sophisticated nucleation strategies; examination of the common crystal orientations in a variety of calcifying organisms reveal that aragonite and calcite single crystals most frequently

DropBooks

nucleate from the *ab* planes. The arrangement of Ca^{2+} ions in this plane (the shortest distance between Ca^{2+} ions is 4.99 Å in calcite, and 4.69 Å in aragonite, respectively; Figure 3) is geometrically not commensurate with the period of amino acid residues in a protein β-strand (approx. 6.9 Å). Moreover, on pointing more or less perpendicular towards the Ca^{2+} ions in the crystal (0 0 1) face, the carboxylate residues of the β-pleated sheet cannot continue the parallel arrangement of planar carbonate anions in the underlying layer(s). The current nucleation model thus does not support the picture of a calcite or aragonite single crystal being nucleated from (0 0 1) crystal faces by virtue of stereochemical selection principles.

Despite the similar positioning of Ca^{2+} ions in the *ab* plane of calcite and aragonite, mollusc shells discriminate between the two polymorphs by secreting them separately in different layers (e.g. prismatic layer and nacre). This suggests that additional factors participate in nucleation. One possibility is that different Mg^{2+} concentrations in the fluids of aragonitic and calcitic layers may be present that could help to shift the balance between the two polymorphs. Another possibility is the presence of polymorph-specific macromolecules that interact with more than one face of the nascent crystal. For a valid explanation of selective nucleation of either polymorph, the current, essentially geometric model will have to be refined. A lot is expected from the first three-dimensional structure of a nucleating macromolecule, although its active conformation may depend on the accompanying insoluble organic matrix in the biological tissues. Finally, novel theoretical approaches are currently being investigated to explore realistic surface properties of the $CaCO_3$ polymorphs which consider surface relaxation as well as hydration of the outermost ionic layers.

Biologically Inspired Engineering of $CaCO_3$ Crystals

Several studies have been directed to the phenomenon of heteroepitaxy in $CaCO_3$ biomineralization. Seminal contributions have come from the group of Mann and co-workers who studied the influence of negatively charged surfactants on crystal nucleation. The group made use of a Langmuir film balance that allows for spreading surfactant molecules as a monolayer at the air–water interface with the charged head groups pointing toward the aqueous subphase. Nucleation of calcite single crystals was observed from monolayers of aliphatic monocarboxylic acids, sulfates or phosphonates. The crystals that grew underneath the monolayers in general showed a significantly narrower size distribution and reduced nucleation time, as compared to calcite crystals precipitated spontaneously from supersaturated solutions. Moreover, the crystals grew crystallographically oriented relative to the monolayer. Calcite single crystals nucleated preferentially from the {10.0} face underneath compressed monolayers of amphiphilic carboxylic acids, while monolayers of alkylsulfates and -phosphonates led to calcite single crystals that nucleated from the (0 0 1) face. Detailed schemes were proposed to rationalize the different modes of interaction between the different head groups of amphiphiles in the monolayers and the corresponding faces from which the crystals were nucleated.

To gain more precise controls over the relative positions of coordinating residues, patterned self-assembled monolayers of bifunctional ω-terminated alkanethiols ($HS(CH_2)_nX$, $X = CO_2^-, SO_3^-, PO_3^{2-}$ and OH) have been produced very recently on different supporting metals (Au, Ag) by means of microcontact printing. Depending on the appropriate combination of functional groups, length of alkyl chains, metal substrate and nucleating area, the selective nucleation of calcite single crystals has been achieved for a huge variety of crystallographic orientations. As a unique feature, the self-assembled monolayers allow one to grow isolated and oriented single crystals with a defined separation which is encoded in the tiling of the nucleating areas. The technique has been further employed to grow crystalline $CaCO_3$ layers that consist of alternating domains of differently oriented calcite single crystals.

The few cited examples demonstrate how model studies may focus on aspects of induced nucleation at organized organic surfaces. Single structural parameters of the organic matrix can be varied systematically and analysed for their influence on crystal nucleation and growth. Results gleaned from these experiments provide important informations that could help to interpret the observed, often highly complex, structures of biominerals. The models studies, furthermore, indicate as to how biologically inspired design and novel technical approaches combine into innovative synthetic strategies for engineering artificial crystalline architectures.

Acknowlegements

The author would like to thank Cia Addadi and Stephen Weiner for valuable discussions. Generous financial support by the MINERVA foundation is gratefully acknowledged.

See also: **II / Crystallization:** Polymorphism. **III / Biological Systems: Ion Exchange Biologically Active Compounds and Xenobiotics: Magnetic Affinity; Supercritical Fluid Crystallization**.

Further Reading

Addadi L and Weiner S (1989) Stereochemical and structural relations between macromolecules and crystals. In: Mann S, Webb J and Williams RJP (eds) *Biomineralization*, pp. 133–156. Weinheim: VCH.

Aizenberg J, Black AJ and Whitesides GM (1999) Oriented growth of calcite controlled by self-assembled monolayers of functionalized alkanethiols supported on gold and silver. *Journal of the American Chemistry Society* 121: 4500–4509.

Briat J-F and Lobréaux S (1998) Iron storage and ferritin in plants. In: Sigel A and Sigel H (eds) *Metal Ions in Biological Systems*, vol. 35, pp. 563–584.

Chasteen ND (1998) Ferritin. Uptake, storage, and release of iron. In: Sigel A and Sigel H (eds) *Metal Ions in Biological Systems*, vol. 35, pp. 479–514.

de Leeuw NH and Parker CS (1998) Surface structure and morphology of calcium carbonate polymorphs calcite, aragonite, and vaterite: an atomistic approach. *Journal of Physical Chemistry B* 102: 2914–2922.

Douglas T and Young M (1998) Host–guest encapsulation of materials by assembled virus protein cages. *Nature* 393: 152–155.

Fendler JH (ed.) (1998) *Nanoparticles and Nanostructured Films: Preparation, Characterization and Applications*. Weinheim: VCH.

Gider S, Awschalom DD, Douglas T *et al.* (1995) Classical and quantum magnetic phenomena in natural and artificial ferritin proteins. *Science* 268: 77–80.

Harrison PM and Arosio P (1996) The ferritins: molecular properties, iron storage function and cellular regulation. *Biochimica et Biophysica Acta – Bioenergetics* 1275: 161–203.

Harrison PM, Hempstead PC, Artymiuk PJ and Andrews SC (1998) Structure–function relationship in the ferritins. In: Sigel A and Sigel H (eds) *Metal Ions in Biological Systems*, vol. 35, pp. 435–477.

Heywood B (1996) Template-directed nucleation and growth of inorganic materials. In: Mann S (ed.) *Biomimetic Materials Chemistry*, pp. 143–173. Weinheim: VCH.

Jambor JL and Dutrizac JE (1998) Occurrence and constitution of natural and synthetic ferrihydrite, a widespread iron oxyhydroxide. *Chemical Reviews* 98: 2549–2585.

Lippmann F (1973) *Sedimentary Carbonate Minerals. Minerals, Rocks and Inorganic Materials*, vol. 6. Berlin: Springer-Verlag.

Lowenstam HA and Weiner S (1989) *On Biomineralization* (Eds Mann, Webb and R.J.P. Williams) New York: Oxford University Press, 7–49.

Möller M and Spatz JP (1997) Mineralization of nanoparticles in block copolymer micelles. *Current Opinion in Colloid and Interface Science* 2: 177–187.

Powell AK (1998) Ferritin. Its mineralization. In: Sigel A and Sigel H (eds) *Metal Ions in Biological Systems*, vol. 35, pp. 515–561.

Schäffer TE, Ionescu-Zanetti C, Proksch R *et al.* (1997) Does abalone nacre form by heteroepitaxial nucleation or by growth through mineral bridges? *Chemistry of Materials* 9: 1731–1740.

Simkiss K and Wilbur KM (1989) Molluscs – Epithelial control of matrix and minerals. In: *Biomineralization. Cell Biology and Mineral Deposition*, pp. 230–260. San Diego: Academic Press.

Weiner S and Addadi L (1997) Design strategies in mineralized biological materials. *Journal of Materials Chemistry* 7: 689–702.

DropBooks

Control of Crystallizers and Dynamic Behaviour

H. J. M. Kramer, Delft University of Technology, Delft, The Netherlands

Copyright © 2000 Academic Press

Introduction

Ideally industrial crystallizers are operated in such a way that the product specifications are met under conditions that permit profitable, trouble-free production of the desired crystalline material. In industrial practice, however, many operational problems can be encountered that reduce the performance of the crystallizer. The most commonly encountered problems are listed here.

- Deposition of crystal solids on the crystallizer internals, often called scaling or fouling. This results in a reduction of the heat transfer in the heat exchanger or leads to plugging of the process lines and can even hamper the flow pattern and thus the mixing in the crystallizer.
- Alternate feed composition. The resulting changes in the level of supersaturation in the crystallizer can lead to nucleation bursts or depletion of secondary nuclei, having a severe effect on the dynamics of the process.
- Disturbances in the heat exchanger in the crystallizer. This leads to variation in the production yield and the crystal concentration, which in turn